Articles

Transthyretin Interacts with Metallothionein 2[†]

I. Gonçalves,[‡] T. Quintela,[‡] G. Baltazar,[‡] M. R. Almeida,[§] M. J. M. Saraiva,[§] and C. R. Santos*,[‡]

Centre of Investigation in Health Sciences—CICS, University of Beira Interior, 6200-506 Covilhã, Portugal, and Molecular Neurobiology, Institute of Molecular and Celular Biology—IBMC, Porto and ICBAS, University of Porto, Rua do Campo Alegre, 823, 4150-180 Porto, Portugal

Received August 14, 2007; Revised Manuscript Received December 20, 2007

ABSTRACT: Transthyretin (TTR) is a 55 kDa homotetrameric protein known for the transport of thyroxine and the indirect transportation of retinol. Within the central nervous system, TTR is primary synthesized and secreted into the cerebral spinal fluid by the choroid plexus (CP), whereas most TTR in the systemic circulation is produced and secreted by the liver. TTR is involved in two types of amyloid disease, the senile systemic amyloidosis and the familial amyloidotic polyneuropathy. TTR has also been implicated in the sequestration of amyloid β peptide (Aβ), preventing its deposition. To explore other biological roles for TTR, we searched for protein−protein interactions using the yeast two-hybrid system with the full-length human TTR cDNA as bait. We found a novel interaction between TTR and metallothionein 2 (MT2) in human liver. This interaction was confirmed by competition binding assays, co-immunoprecipitation, cross-linking, and Western blotting experiments. Binding studies using MT1 showed a saturable specific interaction with TTR with a K_d of 244.8 ± 44.1 nM. Western blotting experiments revealed a TTR−MT1/2 protein complex present in rat CP and kidney tissue extracts. Immunofluorescence experiments, in CP primary cell cultures and in CP paraffin sections, showed co-localization of TTR and MT1/2 in the cytoplasm of epithelial CP cells and localization of MT1/2 in the endoplasmic reticulum. Moreover, dot blot immunoassays of rat CSF provided the first evidence, to our knowledge, of circulating metallothionein in CSF. Taken together, we suggest that TTR−MT1/2 complexes may be functionally significant not only in healthy conditions but also in Aβ deposition in Alzheimer disease, thereby providing a novel potential therapeutic target.

In the proteome era, identification of the function and interactions of disease-associated proteins provides a major opportunity to elucidate disease mechanisms and develop new diagnostic markers and therapeutic targets (*1*).

Transthyretin (TTR[1]) is associated with two amyloid diseases; nonmutated TTR is found in amyloid deposits of patients suffering from senile systemic amyloidosis, whereas a large number of single amino acid substitutions cause familial amyloidotic polyneuropathy, an autosomal dominant neurodegenerative disease (*2*, *3*). TTR is a 55 kDa protein known for the transport of thyroxine (T4) and retinol binding protein (RBP), which is the carrier of vitamin A (retinol). Within the central nervous system (CNS), TTR is primarily synthesized and secreted into cerebrospinal fluid (CSF) by the choroid plexus (CP) where it represents about 20% of the total protein synthesis (*4*, *5*), whereas most TTR in the systemic circulation is produced and secreted by the liver (*6*). TTR is biologically active as a tetramer and can carry two T4 molecules simultaneously and one RBP in vivo (*7*).

In vivo, TTR has other ligands, such as apolipoprotein AI (*8*), lutein (*9*), and norepinephrine oxidation products (*10*). In addition, in vitro binding studies of TTR demonstrated that the protein binds a wide variety of compounds, such as pharmacological agents like penicillin, salicylate, steroids, some nonsteroidal anti-inflammatory drugs (*11*−*14*), environmental pollutants (*15*, *16*), thyromimetic compounds (*17*), some flavenoids (*18*, *19*), and xanthone derivatives (*20*).

It has been suggested that TTR prevents Aβ fibrilization, in particular, TTR present in CSF produced by CP. This hypothesis is supported by the observation that TTR sequesters Aβ, inhibiting the formation of fibrils (*21*−*23*), and by the presence of soluble Aβ in CSF and the serum of normal and AD subjects (*24*). Moreover, a negative correlation between TTR levels and AD progression is strengthened by data arising from human studies (*22*) and murine experimentation (*23*).

[†] This work was supported by Grants POCI/SAU-NEU-55380/2004 (to C. R. Santos) and POCI/SAU/-OBS/ 56929/2004 (to M. J. Saraiva) from Fundação para a Ciência e Tecnologia (Portugal); I. Gonçalves and T. P. Quintela are recipients of postdoctoral (SFRH/BPD/19337/2004) and Ph. D. (SFRH/BD/21765/2005) fellowships, respectively, from Fundação para a Ciência e Tecnologia (Portugal).

* To whom correspondence should be addressed. Tel.: +351 275329044. Fax: +351 275 329 099. E-mail: csantos@fcsaude.ubi.pt.

[‡] University of Beira Interior.

[§] University of Porto.

[1] Abbreviations: TTR, transthyretin; CSF, cerebral spinal fluid; CP, choroid plexus; MT, metallothionein; CNS, central nervous system; Aβ, amyloid β peptide; ER, endoplasmic reticulum.

10.1021/bi7016377 CCC: $40.75
Published on Web 02/01/2008

Together, these observations prompted us to explore other biological roles of TTR, searching for new TTR protein interactions with the yeast two-hybrid system. Using the full-length human TTR cDNA as bait, we partially screened a human liver cDNA library and found a new TTR interactor, metallothionein 2 (MT2). This new interaction is clearly demonstrated in vitro by co-immunoprecipitation, cross-linking experiments, competition binding assays, and Western blotting and in vivo by co-immunolocalization studies.

EXPERIMENTAL PROCEDURES

Yeast Two-Hybrid System. The Matchmaker GAL4 two-hybrid system 3 was obtained from CLONTECH. pGBKT7−TTR, which encodes the full-length human TTR cDNA fused in frame to GAL4 DNA binding domain, was used as bait. The human liver cDNA library, fused with the GAL4-activation domain in the pACT2 vector, was obtained from CLONTECH. The two-hybrid screening was carried out by using yeast strain AH109 transformed with pGBKT7−TTR. Transformants were selected on dropout plates (SD base, $^{-}$trp^{-}leu^{-}ade^{-}his) in the presence of the chromogenic substrate X-α-Gal (5-bromo-4-chloro-3-indolyl-α-D-galactopyranosidose, CLONTECH) for a minimum of 5 days at 30 °C. Approximately 3.6×10^5 colonies were screened, and 59 positive clones were identified. The cDNA inserts of the positive clones were amplified by PCR using primers complementary to the pACT2 vector. Subsequently, the pACT2−cDNA constructs were isolated from positive yeast colonies, as recommended by the supplier, transformed into supercompetent *Escherichia coli* XL1B, grown under selection, reisolated, and analyzed by restriction digests. The purified constructs were then retested with the pGBKT7−TTR bait construct. Positive inserts were sequenced and analyzed by comparison to the GenBank sequence data.

In Vitro Transcription/Translation and Co-immunoprecipitation (Co-IP). The MT2 construct was obtained from the library made in the pACT2 vector, lacking the T7 promoter which was introduced by PCR upstream of HA−MT2, using the following primers: 5′AAA ATT GTA ATA CGA CTC ACT ATA GGG CGA GCC GCC ACC ATG TAC CCA TAC GAC GTT CCA GAT TAC GCT 3′ and 5′ACT TGC GGG GTT TTT CAG TAT CTA CGA T3′. In vitro transcription/translations of T7-HA−MT2 linearized template and the pGBKT7−c-Myc−TTR construct were carried out using the TNT-T7 coupled reticulocyte lysate system (Promega), with [^{35}S]methionine incorporation (>1,000 Ci/mmol at 10 mCi/mL; Amersham-Pharmacia Biotech), according to the manufacturer's instructions. The fusion proteins were analyzed by SDS-PAGE and autoradiography. Co-IP was performed with the HA−MT2 and c-Myc−TTR fusion proteins and HA−Tag polyclonal or c-Myc monoclonal antibody, using a Matchmaker Co-IP kit (BD Biosciences), as per the manufacturer's instructions. Positive controls of Co-IP were performed in parallel with the experiment. Proteins were resolved by SDS-PAGE on a 12% gel, followed by autoradiography.

Radioligand Binding Assays. Recombinant TTR was purified from *Escherichia coli* D1210 transformed with plasmids carrying wild-type TTR cDNA, as described by Almeida et al. (*25*). The same procedure was employed to isolate Cys10Ser TTR. Commercial rabbit liver MT1 was obtained from Sigma (St. Louis, MO). The supplier-reported metal assays of the MT1 sample show ≈7% metals (Cd + Zn) by mass, which indicates complete occupation of all metal-binding sites by cadmium or zinc.

For binding studies, TTR was iodinated with Na^{125}I (NEN) using the Iodogen (Sigma) method, following the supplier's instructions. To a reaction tube coated with 100 μg of Iodogen, 1 mCi, 37 MBq of Na^{125}I was added, followed by 10 μg of TTR in PBS. The reaction was allowed to proceed on ice for 20 min. The iodination mix was subsequently desalted in a 5 mL Sephadex G50 column. Only ^{125}I-TTR that is more than 95% precipitable in trichloroacetic acid was used.

Binding of ^{125}I-TTR to MT1 was carried out in 96 well plates (Maxisorp; Nunc, Rochester, NY) coated overnight with 2 μg/well of MT1. Increasing concentrations of ^{125}I-TTR (as indicated) in binding buffer (0.1% skim milk in minimal essential medium, MEM) were incubated in each well for 2 h at 37 °C with gentle shaking. Unoccupied sites were blocked by addition of 200 μL of 5% nonfat dried milk in PBS for 2 h at 37 °C. We performed three replicas of each sample. Binding was determined after 5 washes with ice cold PBS with 0.05% Tween 20 (0.2 mL/wash). Then, 100 μL of elution buffer (NaCl 0.1 M containing 1% Nonidet P40) was added for 5 min at 37 °C, and the content of the wells (bound TTR) was aspirated and counted in a gamma counter (Wallac, Wizard). Nonspecific binding was determined by incubating similar amounts of labeled ^{125}I-TTR in the wells in the presence of 100× molar excess of nonlabeled (cold) TTR. Specific binding was calculated as the difference between total binding and nonspecific binding. Binding data were fit to a one-site model and analyzed by the method of Klotz and Hunston using nonlinear regression analysis with the Prism program (GraphPad Software Inc.), as previously described (*26*). The results presented are representative of a minimum of two independent experiments.

Animals. Three male Wistar rats were housed in appropriate cages at constant room temperature in a 12 h light/12 h dark cycle and given standard laboratory chow and water ad libitum. Euthanasia was carried under anaesthesia (Clorketam 1000), and the CSF, choroid plexus (CP), and kidney (K) were collected and frozen at −80 °C for protein extraction. Brains including the CP were also fixed in 4% paraformaldehyde for immunohistochemistry. All procedures were performed in compliance with National and European Union regulations for the care and handling of laboratory animals (Directive 86/609/EEC).

Protein Extracts, Electrophoresis, and Western Blot. Kidneys and CPs from both the lateral and fourth ventricle from 3−5 day old rats (both sexes) were dissected under a stereomicroscope and kept in Hank's balanced salt solution (HBSS). After sonication for 5 min, the extracted material was sedimented at 12000*g* for 30 min at 4 °C. Protein concentrations from resulting supernatants were determined by a Bio-Rad protein assay reagent (Bio-Rad, Hercules, CA) according to the manufacturer's directions. The samples were resolved in 12.5% polyacrylamide native or SDS-PAGE gels for 2 h at 150 V. Proteins were transferred to PVDF membrane (Bio-Rad, 0.22 μm) under acidic conditions (0.7% acetic acid) over 4 h at 1000 mA. Membranes were cut in two pieces, one containing human TTR, K, and CP total protein extracts and the other with MT1 and the same protein

extracts. The first half of the membrane was incubated with a rabbit anti-mouse TTR diluted to 1:1000. Alkaline phosphatase conjugated goat anti-rabbit IgG (H + L) linked was used as a secondary antibody (1:20000 dilution). The other half of the membrane was incubated with a mouse monoclonal MT1/2 antibody (Abcam, UC1MT; recognizes MT1 and MT2), diluted to 1:1000, and alkaline phosphatase conjugated goat anti-mouse IgG + IgM (H + L), linked secondary antibody, was diluted to 1:20000. Peptide neutralization of the primary antibody anti-MT was carried out using the same dilution of the antibody and a 10-fold (by weight) excess of MT1 protein in a small volume of PBS. This pre-absorption was carried out overnight at 4 °C. Protein bands were detected using the enhanced chemifluorescence (ECF) system (Amersham Biosciences) and analyzed by densitometric analysis using the Quantity One software (Bio-Rad).

Cross-Linking of TTR to MT. Human recombinant TTR (2μg) was incubated for 1 h at 37 °C with 2 μg of commercial MT1 from rabbit liver (Sigma). The cross-linker bis-(maleimido)ethane (BMOE, Pierce) was prepared 1000-fold concentrated in dimethylsulfoxide and added to the protein sample to a final concentration of 0.2 mM. The reaction mixture was incubated for 1 h at room temperature. The products were boiled for 5 min, separated on a 15% SDS-PAGE, and visualized by silver staining or transferred to PVDF and visualized by human anti-TTR or anti-MT1/2 immunoblotting, as described before.

Primary Cell Culture of Choroidal Epithelial Cells. Animals used in the experiments were anesthetized with 50 μL of Clorketam 1000 before euthanasia. Choroid plexus tissues from both the lateral and fourth ventricles from 3−5 day old rats (both sexes) were dissected under a stereomicroscope and kept in Hank's balanced salt solution (HBSS). The tissues were then digested in HBSS containing 0.2% pronase (Fluka) at 37 °C for 5 min. After centrifugation (500*g* for 5 min), the pellet was collected and resuspended in DMEM medium supplemented (Sigma, St. Louis, MO) with 10% fetal bovine serum (FBS) (Biochrom AG) and 100 units/mL of penicillin/streptomycin (Sigma). Cells were further mechanically dissociated through a 1 mL pipet tip for 1−2 min. Dissociated cells were washed in DMEM with penicillin, streptomycin, and 10% FBS and resuspended in a normal growth medium of DMEM supplemented, in addition to antibiotics and 10% FBS, with 10 ng/mL epidermal growth factor (EGF) (Sigma), 5 μg/mL insulin (Sigma), and 20 μM cytosine arabinoside (Ara-C) (Sigma). The cells were plated and cultured in a humidified incubator with 95% air−5% CO_2 at 37 °C. After the first 2 h of incubation resulting in fibroblast adhesion, supernatants were collected, and nonadherent cells were seeded into 12 mm laminin-coated culture wells (Nunc). The growth medium was replaced 2 days after the initial seeding and every 2−3 days thereafter. A 6−7 day culture was used in co-immunolocalization studies.

Co-immunolocalization. After rinsing, the cells were prefixed in minimal essential medium with a few drops of 4% paraformaldehyde and fixed in 4% paraformaldehyde for 10 min. Cells and choroid plexus paraffin sections (6 μm) were then permeabilized with 1% Triton X-100 in phosphate-buffered saline (PBS) for 10 min and blocked by incubation with 20% FCS in PBS with 0.1% Tween-20 for 60 min at room temperature. Cells were then incubated overnight at 4 °C with the primary antibodies, mouse monoclonal MT1/2 antibody (Abcam; 1:50) and rabbit anti-mouse TTR antibody (1:1000). After washing, the cells were incubated for 60 min, at room temperature, with Alexa Fluor 488 goat anti-rabbit IgG conjugate (Molecular Probes; 1 μg/mL) or with Alexa Fluor 546 goat anti-mouse IgG conjugate (Molecular Probes; 1 μg/mL). To determine if MT1/2 is present in endoplasmic reticulum (ER), CP cells were also incubated with a goat polyclonal MT1/2 antibody (Santa Cruz Biotechnology; 1:50) and with an antibody directed against the ER-associated protein disulfide isomerase raised in a mouse (Molecular Probes, 1:1000) overnight at 4 °C. After washing, the cells were first incubated for 60 min, at room temperature, with Alexa Fluor 350 donkey anti-goat IgG conjugate (Molecular Probes; 1 μg/mL) and then, after the washings, with Alexa Fluor 488 goat anti-mouse IgG conjugate (Molecular Probes; 1 μg/mL). To assess immunostaining specificity, the primary antibody was omitted in some coverslips. Under these conditions, no specific immunofluorescence was detected. Fluorescence was analyzed on a Zeiss inverted microscope.

Dot Blot Experiments. Rat CSFs and rabbit liver MT1, used as positive control, were immobilized in PVDF membranes. Membranes were incubated with mouse monoclonal MT1/2 antibody using the protocol described for Western blotting. Peptide neutralization of anti-MT1/2 was carried out using the protocol described before.

RESULTS

We present several lines of evidence indicating that TTR interacts with MT1/2 in vitro and in vivo.

Detection of the TTR−MT Interaction by Two-Hybrid Screening in Yeast. To identify new proteins that interact with TTR, a fusion construct of the GAL4 DNA-binding domain with full-length TTR cDNA was generated and used as bait for the screening of a human liver yeast two-hybrid cDNA library. Of the 3.6×10^5 transformants screened, 59 cDNA clones grew in the absence of tryptophan, leucine, histidine, and adenine, and α-galactosidase activity was expressed. The pACT2/cDNA plasmids were isolated and retested. After retransformation, 17 independent positive clones were identified and sequenced. A homology search of the GenBank database revealed that seven of these clones encoded human metallothionein 2.

Binding of TTR to MT In Vitro. To characterize the TTR−MT2 interaction, we started by investigating, in vitro, the interaction of TTR with commercially available rabbit liver MT1, a highly conserved mammalian MT isoform. Rabbit liver MT1 contains 92% homology with human MT2. When the concentration of MT1 adsorbed to microtiter wells was held constant (2 μg/well), binding of ^{125}I-TTR was dose-dependent, specific, and saturable, with an apparent K_d of approximately 244.8 ± 44.1 nM (Figure 1A). In an attempt to verify if the TTR−MT1/2 interaction occurs through the thiol group of the only cysteine residue in TTR (residue Cys^{10}), binding assays with a mutant form TTR(Cys10Ser) were carried out. The competition effect of TTR(Cys10Ser) was similar to that of wtTTR, excluding an interaction via disulfide bridges (data not shown).

In Vitro Transcription/Translation and Co-immunoprecipitation. The interaction between TTR and MT was further

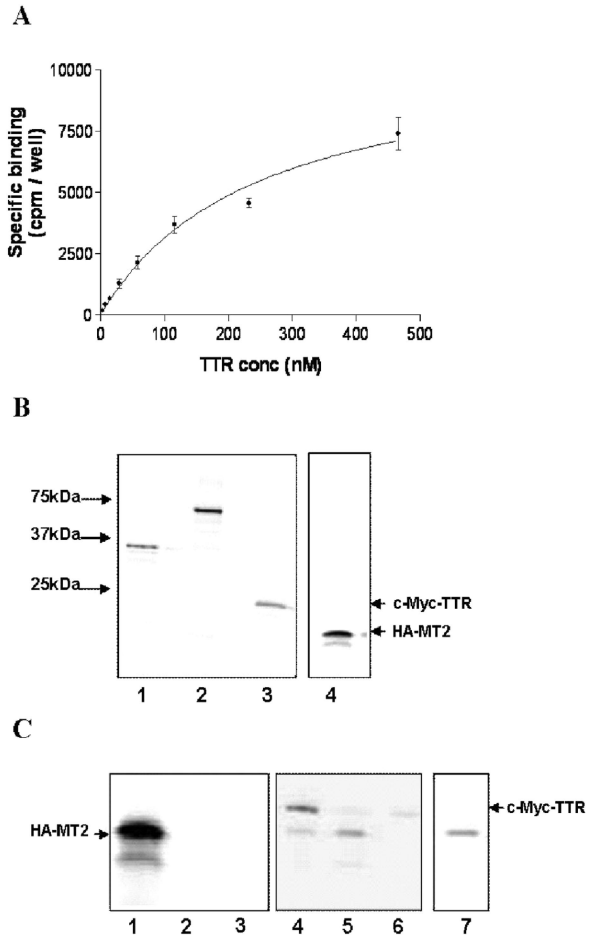

FIGURE 1: In vitro characterization of the TTR−MT interaction. (A) Binding of ^{125}I-TTR to MT immobilized in microtiter wells (2 μg/well). The indicated concentrations of ^{125}I-TTR were added to wells preincubated with MT, and the specific binding was assessed. (B) Autoradiography of the SDS-PAGE analysis of translated [^{35}S]-methionine proteins. Lanes 1 and 2: Co-IP kit control fusion proteins c-Myc−p53 and HA−SV40 large-T antigen; lanes 3 and 4: fusion proteins c-Myc−TTR and HA−MT2. (C) Autoradiography of the SDS-PAGE analysis shows that TTR co-immunoprecipitates with MT2. Lane 1: HA−MT2 protein only; lanes 2 and 3: negative controls of Co-IP (c-Myc−TTR with anti-HA and HA−MT2 with anti-c-Myc); lanes 4 and 5: c-Myc−TTR and HA−MT2 immunoprecipitated with anti-c-Myc and anti-HA, respectively; lanes 6 and 7: positive controls of the Co-IP kit (c-Myc−p53 with anti-c-Myc and HA−SV40 large-T antigen with anti-HA).

characterized by generating Myc and HA fusion proteins using rabbit reticulocyte lysates followed by co-immunoprecipitation (Co-IP). Fusion proteins c-Myc−TTR and HA−MT2 were in vitro transcribed/translated with [^{35}S]methionine incorporation and detected by autoradiography, as shown in Figure 1B. The c-Myc−TTR protein together with HA−MT2 was then immunoprecipitated. When the anti-c-Myc antibody was used for immunoprecipitation, the HA−MT2 protein was coprecipitated (lane 4, Figure 1C). When the anti-HA antibody was used for immunoprecipitation, the c-Myc−TTR protein was coprecipitated (lane 5, Figure 1C), therefore supporting an interaction between TTR and MT2. Negative (lanes 2 and 3, Figure 1C) and positive (lanes 6 and 7, Figure 1C) controls confirmed antibody specificity.

TTR Binds MT in Rat Choroid Plexus and Kidney Tissues. MT1 as well as MT2 has been reported to be ubiquitously expressed in all tissues analyzed to date (*27*), which led us to investigate the presence of TTR−MT complexes in other tissues, where these two proteins coexist. Total protein extracts from the rat choroid plexus and kidney were prepared, and native polyacrylamide gel electrophoresis followed by Western blotting, with anti-TTR and anti-MT1/2 antibodies, were carried out. The monoclonal anti-MT antibody used recognizes both MT1 and MT2 isoforms. As can be seen in Figure 2, an upper band (*) recognized by anti-MT and anti-TTR antibodies was observed in both tissues, with different electrophoretic mobilities from free TTR and MT1 (Figure 2, lower bands). Controls performed with secondary antibodies and with the MT-neutralized antibody confirmed antibody specificity (data not shown). These results are compatible with the existence of TTR−MT1/2 complexes in both tissues.

Cross-Linking of TTR to MT. In order to further demonstrate that TTR interacts with MT1/2, cross-linking experiments with both proteins, using BMOE (Figure 3), were carried out. In silver-stained gels, as seen in lane 3 of Figure 3A, TTR cross-linked with MT1 shows one extra band with an intermediate electrophoretic mobility, compared to the dimeric and monomeric TTR forms (indicated by an arrow). To better elucidate these observations, we performed immunodetection for both TTR and MT1 (Figure 3B). As in silver-stain detection, the observed extra band resulting from TTR cross-linked to MT1 incubated with human anti-TTR (Figure 3B, lane 3) is different from the bands obtained with TTR alone and with cross-linked TTR alone (Figure 3B, lanes 1 and 2). The MT immunoblot of TTR cross-linked with MT1 (Figure 3B, lane 6) revealed also an extra band (indicated by an arrow) with the same electrophoretic mobility as the band observed in lane 3 detected with the anti-TTR antibody. MT1 alone and cross-linked MT1 alone are shown in lanes 4 and 5, respectively (Figure 3B), further sustaining an interaction between both proteins where MT1 appears to bind the monomeric form of TTR.

Co-localization of TTR and MT. To co-localize TTR and MT in vivo, we performed double staining of MT1/2 and TTR. For this purpose, rat primary cell cultures from choroidal epithelial cells were established, and rat CP paraffin sections were prepared. Immunofluorescence staining was performed using MT1/2 and TTR antibodies followed by incubation with anti-mouse and anti-rabbit Alexa Fluor secondary antibodies, respectively (Figure 4). MT was localized throughout the cytoplasm and the nucleus, whereas TTR was localized in the cytoplasm only. For co-localization analysis, images of MT (red channel) and TTR (green channel) were digitally merged using 25 Software, release 4.4(Carl Zeiss Imaging Systems). MT and TTR were co-localized in the cytoplasm, particularly in the perinuclear area as shown by yellow areas in the merged image (Figure 4A and B). The presence of MT in the ER shown by the yellow areas in Figure 4C strongly suggests that co-localization occurs in this cellular compartment, where TTR is also present.

CSF Dot Blot Experiments. All of the obtained results prompt us to hypothesize that, like TTR, MT1/2 would also be present in CSF. To test this hypothesis, we searched for MT in three different rat CSFs samples by dot blot experiments incubated with anti-MT1/2 antibody. As we can see in Figure 5, the obtained results clearly demonstrate that MT1/2 is present in rat CSF. In order to exclude nonspecific binding of the MT antibody to rat immunoglobulins, we have

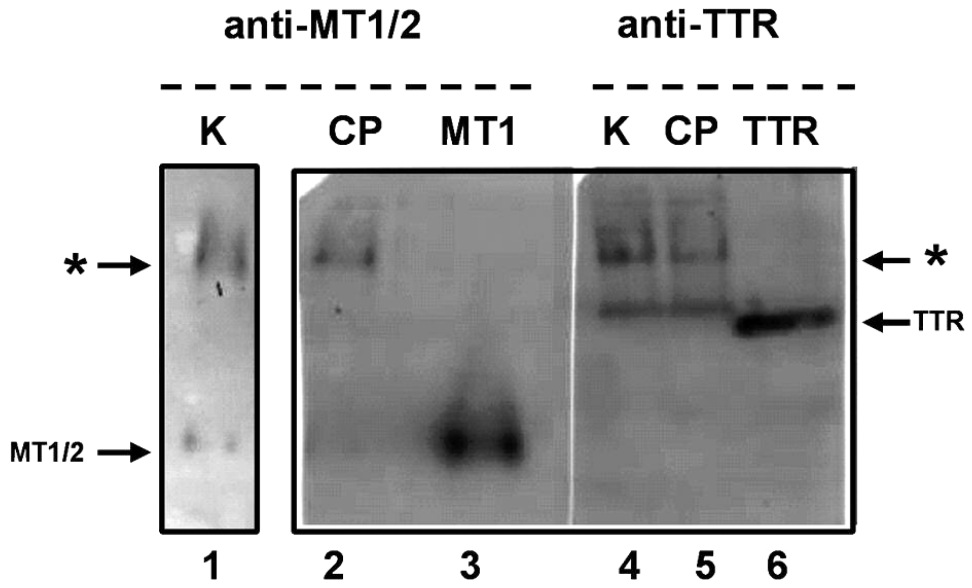

FIGURE 2: Anti-MT1/2 and anti-TTR immunoblot analysis under native conditions of total protein extracts from rat kidney (K) and choroid plexus (CP). Lanes 1 and 4: 30 μg of rat kidney protein extract; lanes 2 and 5: 30 μg of rat CP protein extract; lanes 3 and 6: 1 μg of pure MT1 and 1 μg of pure TTR, respectively. The upper arrows indicate the complex TTR bound to MT1 (*). The lower arrows indicate free MT1 and free TTR.

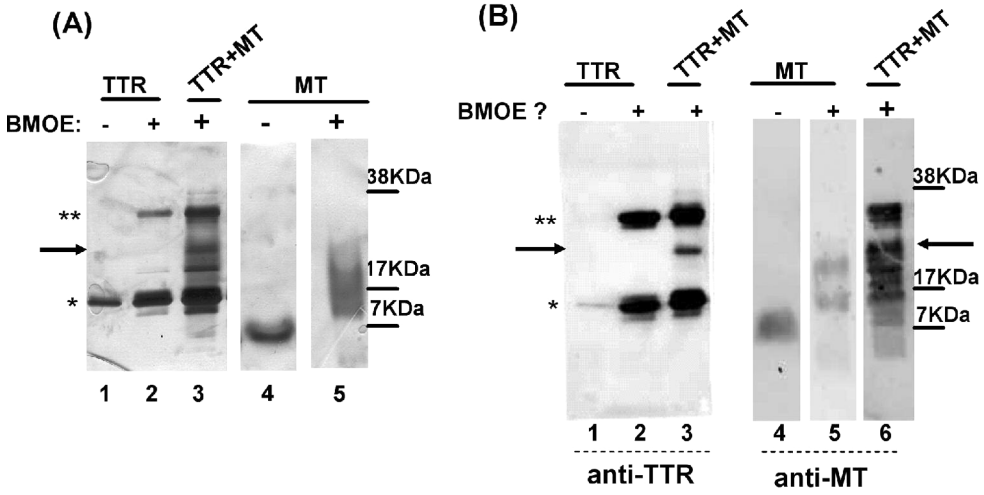

FIGURE 3: Cross-linking of TTR to MT1 with BMOE, analyzed in 15% SDS-PAGE. Arrows indicate the TTR−MT cross-linked species; * and ** indicate the TTR monomer and dimer, respectively. (A) Silver-stain detection. Lanes 1 and 2: TTR without and with BMOE; lane 3: TTR cross-linked to MT1 with BMOE; lanes 4 and 5: MT1 without and with BMOE. (B) Western blot detection of TTR cross-linked to MT1 with BMOE. Anti-TTR- lanes 1 and 2: TTR without and with BMOE; lane 3: TTR cross-linked to MT1 with BMOE. Anti-MT- lanes 4 and 5: MT1 without and with BMOE; lane 6: TTR cross-linked to MT1 with BMOE.

carried out MT1/2 neutralization of the primary antibody against MT, and in this situation, no dots were detected in the CSF.

DISCUSSION

The focus of our research was to identify new ligand TTR interactors to better understand its role in normal physiology and in pathological conditions such as amyloid deposition, in TTR amyloidoses, as well as in AD. We searched for TTR-associated proteins by a yeast two-hybrid system using TTR cDNA as bait. While screening a human liver cDNA library, we identified MT2 as a putative TTR-associated protein. However, the yeast two-hybrid system provides only potential interactions that have to be confirmed by further biological experimentation (*28*). Therefore, to test the TTR−MT2 interaction, we performed co-immunoprecipitation, competition binding assays, Western blotting and cross-linking experiments in vitro, and co-localization of the two proteins in vivo using double immunofluorescence. The affinity of TTR to MT1/2 is relatively high, with a K_d of 244.8 ± 44.1 nM, the same order of magnitude as that previously reported for other TTR ligands (K_d[TTR−RBP] = 800 nM; K_d[TTR−T4] = 10nM) (*29*). The results obtained in competition binding assays with the mutant TTR-(Cys10Ser) and wtTTR showed similar competition effects, demonstrating that Cys^{10} residue is not involved in TTR−MT1/2 interaction, therefore excluding an interaction via disulfide bonding. Western blot studies under native conditions showed TTR−MT1/2 complexes in rat CP and kidney. Immunoblotting using both the anti-MT and the anti-TTR antibodies in samples containing TTR and MT cross-linked by BMOE detects a molecular weight protein complex which has an electrophoretic mobility between the TTR monomer

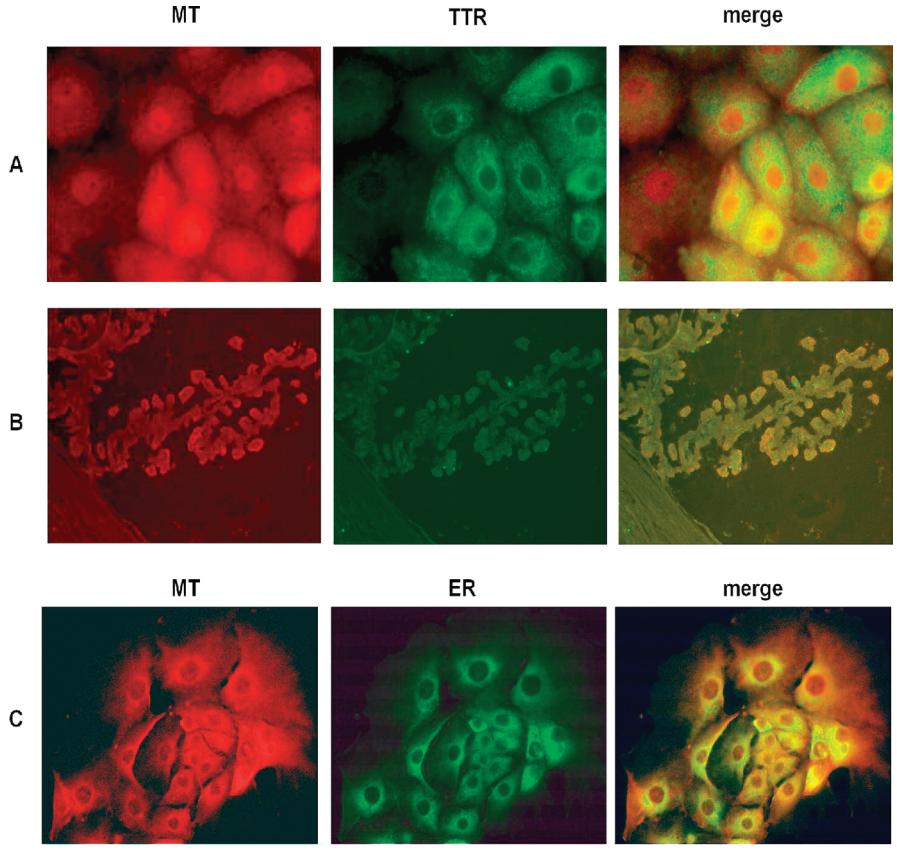

FIGURE 4: Immunofluorescence microscopy of MT1/2 co-localization with TTR and ER. (A) Rat CP primary cell cultures (63×); (B) paraffin sections of rat CP (20×). Both cells and CP sections were stained with a mouse monoclonal MT1/2 antibody followed by Alexa Fluor 546 goat anti-mouse IgG conjugate (red) and a rabbit polyclonal TTR antibody followed by Alexa Fluor 488 goat anti-rabbit IgG conjugate (green). (C) Rat CP primary cell cultures (63×) stained with a goat polyclonal MT1/2 antibody and with an antibody directed against the ER-associated protein disulfide isomerase raised in mouse followed by incubation with Alexa Fluor 350 donkey anti-goat IgG conjugate (red) and Alexa Fluor 488 goat anti-mouse IgG conjugate (green). Co-localization of MT/TTR and MT/ER corresponds to the yellow areas in merged images.

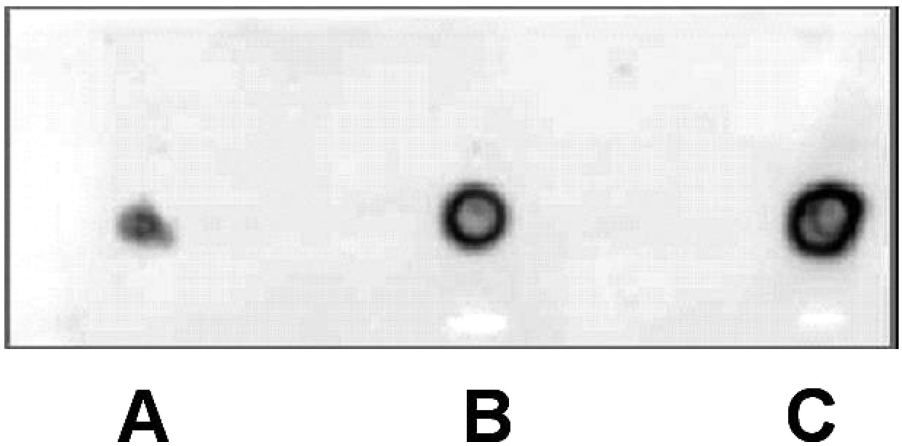

FIGURE 5: Anti-metallothionein immunoblot analysis of membrane-immobilized rat CSF. (A) 1 μg of rabbit liver MT1; (B) 10 μL of rat CSF; (C) 15 μL of rat CSF.

and dimer, suggesting that MT binds the monomer of TTR but not dimers nor tetramers. In vivo experiments, with double immunostaining of MT1/2 and TTR, demonstrated co-localization of these proteins in the cytoplasm of CP cells and in CP tissue sections. Moreover, the presence of MT1/2 in the ER strongly suggests that TTR and MT1/2 co-localize in this cellular compartment. Despite the fact that co-localization does not mean the existence of a complex, the simultaneous presence of both proteins in the ER and the detection of TTR−MT complexes in the CSF suggest that should a complex exist, it may localize in the secretory pathway of CP cells or it may form outside of the cell in the CSF. TTR synthesized by CP is released into the CSF, and we have detected MT1/2 in CSFs from rats, which is likely to be secreted by CP as well. Actually, MTs have been found in both intracellular compartments and in extracellular spaces. Although the presence of MT outside of the cells has been linked to stressful conditions, the process of its release is not yet well-clarified. Lynes et al. (*30*) suggested that MT may be selectively released, and the pool of extracellular

MT may represent an important regulator of various cellular functions.

Regarding the presence of TTR−MT complexes in the kidney, as demonstrated by Western blotting in native conditions, these are likely to localize in renal tubes that reuptake TTR (*31*) and where MT1/2 is also present (*32*). Taken together, both in vivo and in vitro experiments support the existence of an interaction between TTR and MT1/2.

Metallothioneins are a family of low molecular weight metal-binding proteins with high cysteine content (*33*) present in multiple isoforms. The isoforms MT1 and MT2, expressed in all organs, are involved in the homeostasis of essential trace metals such as zinc and copper and protect from the toxic effects following heavy-metal exposure (*27*). MT1/2 in the central and peripheral nervous system display neuroprotective actions and inhibit delayed damage such as oxidative stress and degeneration (*34*−*36*). Strong correlations have been drawn around MT1/2 and the onset and progression of neurodegenerative diseases. Elevated MT1/2 expression is observed in Alzheimer's, Parkinson's, multiple sclerosis, and motor neuron diseased patients (*34*−*36*). Impaired zinc homeostasis, via MT, has been linked to many age-related brain dysfunctions including AD; Aβ displays binding sites for Zn^{2+}, and Zn^{2+} binding promotes Aβ deposition in amyloid plaques (*37*). The major in vivo evidence supporting the involvement of Zn^{2+} in AD comes from the results obtained by crossing Tg2576 transgenic mice (expressing cerebral amyloid plaque pathology) with ZNT3 (brain zinc transporter protein) knockout mice. This new strain displays a markedly reduced plaque load and less insoluble Aβ as compared with that of Tg2576 mice (*38*), indicating that the availability of Zn^{2+} contributes predominantly to Aβ deposition in the Tg2576 mice model of AD.

Concurrently, several reports in the literature describe TTR as an Aβ protein scavenger (*21*−*24*). There is increasing evidence that TTR negatively correlates with Aβ levels and senile plaque abundance in AD patients (*22*, *39*) probably due to the ability of TTR to form complexes with Aβ, preventing the formation of amyloid fibrils (*21*, *40*, *41*). More recently, Choi et al. (*42*) demonstrated that Aβ levels and deposition are elevated in the brains of *ceAPPswe/PS1*Δ*E9/TTR*+/− mice (AD model of transgenic mice crossed to TTR null mice) compared to age-matched *ceAPPswe/PS1*Δ*E9/TTR*+/+ mice, further stressing the importance of TTR in this process.

The existence of an interaction between two proteins involved in the modulation of Aβ levels, which are both present in CP and CSF, highlights the importance of further understanding how the interaction herein described may affect the role of each protein on Aβ deposition. Moreover, the preferential binding of MT to the TTR monomer may have implications in TTR amyloid formation, which is the main cause of senile systemic amyloidosis, a late onset cardiomyopathy, where amyloid deposits are composed of wild-type TTR and familial amyloiditic polyneuropathy where these are composed by mutated TTR variants, which are prone to undergo fibrilization earlier in adulthood (*2*, *43*).

REFERENCES

1. Blackstock, W. P., and Weir, M. P. (1999) Proteomics: quantitative and physical mapping of cellular proteins, *Trends Biotechnol. 17*, 121−127.
2. Saraiva, M. J. (2001) Transthyretin amyloidosis: a tale of weak interactions, *FEBS Lett. 498*, 201−203.
3. Cornwell, G. G., III, Sletten, K., Johansson, B., and Westermark, P. (1988) Evidence that the amyloid fibril protein in senile systemic amyloidosis is derived from normal prealbumin, *Biochem. Biophys. Res. Commun. 154*, 648−653.
4. Schreiber, G., Aldred, A. R., Jaworowski, A., Nilsson, C., Achen, M. G., and Segal, M. B. (1990) Thyroxine transport from blood to brain via transthyretin synthesis in choroid plexus, *Am. J. Physiol. 258*, R338−345.
5. Herbert, J., Wilcox, J. N., Pham, K. T., Fremeau, R. T., Jr., Zeviani, M., Dwork, A., Soprano, D. R., Makover, A., Goodman, D. S., Zimmerman, E. A., et al. (1986) Transthyretin: a choroid plexus-specific transport protein in human brain. The 1986 S. Weir Mitchell award, *Neurology 36*, 900−911.
6. Felding, P., and Fex, G. (1982) Cellular origin of prealbumin in the rat, *Biochim. Biophys. Acta 716*, 446−449.
7. Monaco, H. L. (2000) The transthyretin-retinol-binding protein complex, *Biochim. Biophys. Acta 1482*, 65−72.
8. Sousa, M. M., Berglund, L., and Saraiva, M. J. (2000) Transthyretin in high density lipoproteins: association with apolipoprotein A-I, *J. Lipid Res. 41*, 58−65.
9. Pettersson, T., Ernstrom, U., Griffiths, W., Sjovall, J., Bergman, T., and Jornvall, H. (1995) Lutein associated with a transthyretin indicates carotenoid derivation and novel multiplicity of transthyretin ligands, *FEBS Lett. 365*, 23−26.
10. Boomsma, F., Man in 't Veld, A. J., and Schalekamp, M. A. (1991) Not norepinephrine but its oxidation products bind specifically to plasma proteins, *J. Pharmacol. Exp. Ther. 259*, 551−557.
11. Munro, S. L., Lim, C. F., Hall, J. G., Barlow, J. W., Craik, D. J., Topliss, D. J., and Stockigt, J. R. (1989) Drug competition for thyroxine binding to transthyretin (prealbumin): comparison with effects on thyroxine-binding globulin, *J. Clin. Endocrinol. Metab. 68*, 1141−1147.
12. Miroy, G. J., Lai, Z., Lashuel, H. A., Peterson, S. A., Strang, C., and Kelly, J. W. (1996) Inhibiting transthyretin amyloid fibril formation via protein stabilization, *Proc. Natl. Acad. Sci. U.S.A. 93*, 15051−15056.
13. Peterson, S. A., Klabunde, T., Lashuel, H. A., Purkey, H., Sacchettini, J. C., and Kelly, J. W. (1998) Inhibiting transthyretin conformational changes that lead to amyloid fibril formation, *Proc. Natl. Acad. Sci. U.S.A. 95*, 12956−12960.
14. Cavalieri, R. R., and Pitt-Rivers, R. (1981) The effects of drugs on the distribution and metabolism of thyroid hormones, *Pharmacol. Rev. 33*, 55−80.
15. McKinney, J. D., Chae, K., Oatley, S. J., and Blake, C. C. (1985) Molecular interactions of toxic chlorinated dibenzo-*p*-dioxins and dibenzofurans with thyroxine binding prealbumin, *J. Med. Chem. 28*, 375−381.
16. Lans, M. C., Klasson-Wehler, E., Willemsen, M., Meussen, E., Safe, S., and Brouwer, A. (1993) Structure-dependent, competitive interaction of hydroxy-polychlorobiphenyls, -dibenzo-*p*-dioxins and -dibenzofurans with human transthyretin, *Chem.-Biol. Interact. 88*, 7−21.
17. Davis, P. J., Cody, V., Davis, F. B., Warnick, P. R., Schoenl, M., and Edwards, L. (1987) Competition of milrinone, a non-iodinated cardiac inotropic agent, with thyroid hormone for binding sites on human serum prealbumin (TBPA), *Biochem. Pharmacol. 36*, 3635−3640.
18. Koehrle, J., Auf'mkolk, M., Spanka, M., Irmscher, K., Cody, V., and Hesch, R. D. (1986) Iodothyronine deiodinase is inhibited by plant flavonoids, *Prog. Clin. Biol. Res. 213*, 359−371.
19. Lueprasitsakul, W., Alex, S., Fang, S. L., Pino, S., Irmscher, K., Kohrle, J., and Braverman, L. E. (1990) Flavonoid administration immediately displaces thyroxine (T4) from serum transthyretin, increases serum free T4, and decreases serum thyrotropin in the rat, *Endocrinology 126*, 2890−2895.
20. Maia, F., Almeida Mdo, R., Gales, L., Kijjoa, A., Pinto, M. M., Saraiva, M. J., and Damas, A. M. (2005) The binding of xanthone derivatives to transthyretin, *Biochem. Pharmacol. 70*, 1861−1869.
21. Schwarzman, A. L., Gregori, L., Vitek, M. P., Lyubski, S., Strittmatter, W. J., Enghilde, J. J., Bhasin, R., Silverman, J., Weisgraber, K. H., Coyle, P. K., Zagorski, M. G., Talafous, J., Eisenberg, M., Saunders, A. M., Roses, A. D., and Goldgaber,

D. (1994) Transthyretin sequesters amyloid beta protein and prevents amyloid formation, *Proc. Natl. Acad. Sci. U.S.A. 91*, 8368−8372.
22. Serot, J. M., Christmann, D., Dubost, T., and Couturier, M. (1997) Cerebrospinal fluid transthyretin: aging and late onset Alzheimer's disease, *J. Neurol., Neurosurg. Psychiatry 63*, 506−508.
23. Stein, T. D., and Johnson, J. A. (2002) Lack of neurodegeneration in transgenic mice overexpressing mutant amyloid precursor protein is associated with increased levels of transthyretin and the activation of cell survival pathways, *J. Neurosci. 22*, 7380−7388.
24. Ghiso, J., Matsubara, E., Koudinov, A., Choi-Miura, N. H., Tomita, M., Wisniewski, T., and Frangione, B. (1993) The cerebrospinal-fluid soluble form of Alzheimer's amyloid beta is complexed to SP-40,40 (apolipoprotein J), an inhibitor of the complement membrane-attack complex, *Biochem. J. 293 (Part 1)*, 27−30.
25. Almeida, M. R., Damas, A. M., Lans, M. C., Brouwer, A., and Saraiva, M. J. (1997) Thyroxine binding to transthyretin Met 119. Comparative studies of different heterozygotic carriers and structural analysis, *Endocrine 6*, 309−315.
26. Sousa, M. M., Yan, S. D., Stern, D., and Saraiva, M. J. (2000) Interaction of the receptor for advanced glycation end products (RAGE) with transthyretin triggers nuclear transcription factor kB (NF-kB) activation, *Lab. Invest. 80*, 1101−1110.
27. Coyle, P., Philcox, J. C., Carey, L. C., and Rofe, A. M. (2002) Metallothionein: the multipurpose protein, *Cell. Mol. Life Sci. 59*, 627−647.
28. Ito, T., Tashiro, K., Muta, S., Ozawa, R., Chiba, T., Nishizawa, M., Yamamoto, K., Kuhara, S., and Sakaki, Y. (2000) Toward a protein−protein interaction map of the budding yeast: A comprehensive system to examine two-hybrid interactions in all possible combinations between the yeast proteins, *Proc. Natl. Acad. Sci. U.S.A. 97*, 1143−1147.
29. Raghu, P., and Sivakumar, B. (2004) Interactions amongst plasma retinol-binding protein, transthyretin and their ligands: implications in vitamin A homeostasis and transthyretin amyloidosis, *Biochim. Biophys. Acta 1703*, 1−9.
30. Lynes, M. A., Zaffuto, K., Unfricht, D. W., Marusov, G., Samson, J. S., and Yin, X. (2006) The physiological roles of extracellular metallothionein, *Exp. Biol. Med. (Maywood, NJ, U.S.) 231*, 1548−1554.
31. Sousa, M. M., Norden, A. G., Jacobsen, C., Willnow, T. E., Christensen, E. I., Thakker, R. V., Verroust, P. J., Moestrup, S. K., and Saraiva, M. J. (2000) Evidence for the role of megalin in renal uptake of transthyretin, *J. Biol. Chem. 275*, 38176−38181.
32. Murakami, M., Tohyama, C., Sano, K., Kawamura, R., and Kubota, K. (1983) Autoradiographical studies on the localization of metallothionein in proximal tubular cells of the rat kidney, *Arch. Toxicol. 53*, 185−192.
33. Kagi, J. H., and Hunziker, P. (1989) Mammalian metallothionein, *Biol. Trace Elem. Res. 21*, 111−118.
34. Hidalgo, J., Aschner, M., Zatta, P., and Vasak, M. (2001) Roles of the metallothionein family of proteins in the central nervous system, *Brain Res. Bull 55*, 133−145.
35. Penkowa, M. (2006) Metallothionein I + II expression and roles during neuropathology in the CNS, *Dan. Med. Bull. 53*, 105−121.
36. West, A. K., Chuah, M. I., Vickers, J. C., and Chung, R. S. (2004) Protective role of metallothioneins in the injured mammalian brain, *Rev. Neurosci. 15*, 157−166.
37. Huang, X., Atwood, C. S., Moir, R. D., Hartshorn, M. A., Vonsattel, J. P., Tanzi, R. E., and Bush, A. I. (1997) Zinc-induced Alzheimer's Abeta1-40 aggregation is mediated by conformational factors, *J. Biol. Chem. 272*, 26464−26470.
38. Lee, J. Y., Cole, T. B., Palmiter, R. D., Suh, S. W., and Koh, J. Y. (2002) Contribution by synaptic zinc to the gender-disparate plaque formation in human Swedish mutant APP transgenic mice, *Proc. Natl. Acad. Sci. U.S.A. 99*, 7705−7710.
39. Merched, A., Serot, J. M., Visvikis, S., Aguillon, D., Faure, G., and Siest, G. (1998) Apolipoprotein E, transthyretin and actin in the CSF of Alzheimer's patients: relation with the senile plaques and cytoskeleton biochemistry, *FEBS Lett. 425*, 225−228.
40. Mazur-Kolecka, B., Frackowiak, J., and Wisniewski, H. M. (1995) Apolipoproteins E3 and E4 induce, and transthyretin prevents accumulation of the Alzheimer's beta-amyloid peptide in cultured vascular smooth muscle cells, *Brain Res. 698*, 217−222.
41. Schwarzman, A. L., Tsiper, M., Gregori, L., Goldgaber, D., Frakowiak, J., Mazur-Kolecka, B., Taraskina, A., Pchelina, S., and Vitek, M. P. (2005) Selection of peptides binding to the amyloid b-protein reveals potential inhibitors of amyloid formation, *Amyloid 12*, 199−209.
42. Choi, S. H., Leight, S. N., Lee, V. M., Li, T., Wong, P. C., Johnson, J. A., Saraiva, M. J., and Sisodia, S. S. (2007) Accelerated Abeta deposition in APPswe/PS1deltaE9 mice with hemizygous deletions of TTR (transthyretin), *J. Neurosci. 27*, 7006−7010.
43. Buxbaum, J. N. (2004) The systemic amyloidoses, *Curr. Opin. Rheumatol. 16*, 67−75.

BI7016377